National Institutes of Health
Turning Discovery Into Health

NIHMS PDF Receipt

Journal title:	The Journal of Immunology
Manuscript title:	Human Eosinophils Express a Distinct Gene Expression Program in Response to IL-3 Compared to Common Beta-Chain Cytokines IL-5 and GM-CSF
Submitter:	American Association Of Immunologists
NIHMSID:	1529962

Manuscript Files

Type	Label	File Name	Upload Date
Manuscript	1	article_1.docx	2019-05-21 05:34:04
Figure	1	figure_1.tif	2019-05-21 05:34:04
Figure	2	figure_2.tif	2019-05-21 05:34:04
Figure	3	figure_3.tif	2019-05-21 05:34:04
Figure	4	figure_4.tif	2019-05-21 05:34:04
Figure	5	figure_5.tif	2019-05-21 05:34:04
Table	1	table_1.doc	2019-05-21 05:34:04
Supplementary Data	1	supp_info_1.xls	2019-05-21 05:34:04
Supplementary Data	2	supp_info_2.xls	2019-05-21 05:34:04
Supplementary Data	3	supp_info_3.xls	2019-05-21 05:34:04
Supplementary Data	4	supp_info_4.xls	2019-05-21 05:34:04

Human Eosinophils Express a Distinct Gene Expression Program in Response to IL-3 Compared to Common Beta-Chain Cytokines IL-5 and GM-CSF

Running Title: Eosinophil β-chain cytokine differential gene expression

Ryan K. Nelson,[*†] Howard Brickner,[*†] Bharat Panwar,[†] Ciro Ramirez Suastegui,[†] Sara Herrera de la Mata,[†] Neiman Liu,[*†] Damaris Diaz,[*†] Laura E. Crotty Alexander,[*‡] Ferhat Ay,[†§] Pandurangan Vijayanand,[†] Grégory Seumois,[†¶] and Praveen Akuthota MD[*†¶]

[*] University of California San Diego; Division of Pulmonary, Critical Care, and Sleep Medicine; La Jolla, CA 92093, USA.

[†] La Jolla Institute for Immunology; La Jolla, CA 92037, USA.

[‡] Veterans Affairs San Diego Healthcare System; La Jolla, CA 92161, USA.

[§] University of California San Diego; School of Medicine; La Jolla, CA 92093, USA.

[¶] G.S. and P.A. are joint senior authors

Corresponding Author:

Praveen Akuthota, MD

Telephone: 858-822-4106

Fax: 858-657-5021

Email: pakuthota@ucsd.edu

Abstract

Despite recent advances in asthma management with anti-IL-5 therapies, many patients with eosinophilic asthma remain poorly controlled. IL-3 shares a common beta subunit receptor with both IL-5 and GM-CSF, but through alpha subunit-specific properties, uniquely influences eosinophil biology and may serve as a potential therapeutic target. We aimed to globally characterize the transcriptomic profiles of GM-CSF, IL-3 and IL-5 stimulation on human circulating eosinophils and identify differences in gene expression using advanced statistical modeling. Human eosinophils were isolated from the peripheral blood of healthy volunteers and stimulated with either GM-CSF, IL-3 or IL-5 for 48 hours. RNA was then extracted and bulk sequencing performed. DESeq analysis identified differentially expressed genes and weighted gene co-expression network analysis independently defined modules of genes that are highly co-expressed. GM-CSF, IL-3 and IL-5 commonly upregulated 252 genes and downregulated 553 genes, producing a pro-inflammatory and survival phenotype that was predominantly mediated through TWEAK signaling. IL-3 stimulation yielded the most numbers of differentially expressed genes that were also highly co-expressed (n = 119). These genes were enriched in pathways involving JAK/STAT signaling. GM-CSF and IL-5 stimulation demonstrated redundancy in eosinophil gene expression. In conclusion, IL-3 produces a distinct eosinophil gene expression program among the beta-chain receptor cytokines. IL-3 upregulated genes may provide a foundation for research into therapeutics for patients with eosinophilic asthma who do not respond to anti-IL-5 therapies.

Key Points

1. Beta-chain receptor cytokines produce a pro-inflammatory and survival phenotype

2. IL-3 stimulation yields a distinct eosinophil gene expression program

3. IL-3-upregualted “hub genes” may have implications in future asthma therapeutics

Keywords: Human, Eosinophils, Cytokines, IL-3, Asthma

Introduction

Asthma is a chronic disease of the airway associated with significant morbidity. In the United States alone, costs related to asthma have amounted to more than eighty billion dollars annually [1]. While a significant proportion of asthmatics maintain control via inhaled corticosteroid therapy, disease heterogeneity has caused many individuals to remain poorly controlled with either high symptom scores and/or frequent exacerbations. The recent approval of monoclonal antibodies against IL-5 has improved control of severe asthmatics with eosinophilia, demonstrating lower exacerbation rates, reduced oral glucocorticoid use, improved lung function, and improved asthma control scores in randomized control trials [2-3]. Nevertheless, not all patients with eosinophilic asthma respond to anti-IL-5 therapies clinically, and populations of functional eosinophils have been shown to remain in the airway despite anti-IL-5 treatment [4-5]. It has therefore been suggested that alternative mechanisms remain relevant to the pathogenesis of eosinophilic asthma in certain individuals and that further investigation is necessary to optimize precision treatment strategies.

One area of investigative focus has involved the cytokines IL-3 and GM-CSF. Similar to IL-5, these two cytokines are produced as part of the Th2 inflammatory response and are crucial to eosinophil development and function [6-7]. Despite all three cytokines sharing a common beta (β)-chain receptor subunit, each differentially affects eosinophil biology as the result of divergent downstream intracellular signaling events through alpha (α)-chain subunit-specific properties [6,8]. Of these cytokines, IL-3 has been shown to most strongly and differentially affect eosinophil function, especially over prolonged stimulation periods [6]. This, together with the observation that eosinophils recruited to the airway following allergen challenge have increased surface levels of the α-chain subunit specific to IL-3 but reduced levels of the α-chain subunit

specific to IL-5, has made IL-3 an attractive potential target in asthma therapeutics [5,9]. While knowledge of eosinophil biology as it relates to IL-3 stimulation has been rapidly growing, no study to date has utilized large scale gene expression profiling to define the IL-3 signature in eosinophils. In the present work, we utilize whole transcriptome bulk RNA sequencing methods and advanced statistical modeling to demonstrate a unique transcriptional profile of human blood eosinophils stimulated by IL-3 *ex vivo* after being harvested from normal subjects. Since IL-3 has been previously described to prolong intracellular signaling in eosinophils [6], we specifically report results following cytokine stimulation for 48 hours.

Materials and Methods

Subject characteristics

Venous blood specimens were obtained after informed consent under a protocol approved by the Institutional Review Board at the University of California San Diego. Whole blood (160 ml) was drawn from 13 healthy volunteers without known allergic disease (7 for gene expression studies and 6 for flow cytometry experiments).

Eosinophil isolation and stimulation

Eosinophils were purified from the peripheral blood of normal donors by negative selection (StemCell Technologies, Vancouver, Canada) as previously described [10]. Briefly, red blood cells (RBCs) were depleted by hetastarch incubation followed by gravity separation. Granulocytes were isolated by centrifugation of RBC-depleted blood over a Ficoll gradient. Eosinophils were then isolated from the granulocyte fraction by incubation with a cocktail of negative selection antibodies followed by passage over a magnetized column. Eosinophil purity was routinely > 99% by Hema 3 staining (Fisher Scientific, Medford, MA), and eosinophil viability was routinely > 99% by trypan blue exclusion after cell isolation. Purified eosinophils from each donor were split equally into unstimulated, GM-CSF-stimulated, IL-3-stimulated, and IL-5-stimulated groups (1-2x10^6 eosinophils per group). Human recombinant IL-3, IL-5 (R&D Systems, Minneapolis, MN) and GM-CSF (BioLegend, San Diego, CA) were used for stimulation, all for 48 hours at a concentration of 10 ng/ml in RPMI-1640 (supplemented with 10% FBS and 1% penicillin/streptomycin) at 37 ˚C. Cell viability remained > 90% for all conditions after 48 hours of stimulation, as assessed by propidium iodide staining. For gene expression experiments, eosinophils were resuspended in a phenol/guanidine-based lysis reagent (QIAzol, Qiagen), either immediately after purification for unstimulated cells or after 48 hours of

stimulation, and stored at -80 ˚C prior to RNA extraction. For flow cytometry experiments, unstimulated eosinophils were stored at 4 ˚C prior to staining, and stimulated cells were stained after 48 hours. Unstimulated eosinophils remained > 98% viable after storage at 4 ˚C for 48 hours.

RNA extraction

Isolated and stimulated eosinophils from 7 donors were stored in QIAzol lysis reagent as previously described. Total RNA was isolated using miRNeasy micro kit (Qiagen) loaded on an automated platform (Qiacube, Qiagen). Samples were quantified as described previously [11-12] and quality of RNA assessed by Fragment Analyzer (Advance Analytical). All samples had an RNA integrity number (RIN) > 8.0 and passed our quality and quantity control steps as described previously [12-13].

mRNA sequencing library preparation

Purified total RNA (≈5 ng) was amplified following the Smart-seq2 protocol [13-14]. Briefly, mRNA was captured using poly-dT oligos and directly reverse-transcribed into full-length cDNA using the described template-switching oligo [13-14]. cDNA was amplified by PCR for 14-15 cycles and purified using AMPure XP magnetic bead (0.9:1 (vol:vol) ratio, Beckman Coulter). From this step, for each sample, 1 ng of cDNA was used to prepare a standard NextEra XT sequencing library (NextEra XT DNA library prep kit and index kits; Illumina). Barcoded Illumina sequencing libraries (Nextera; Illumina) were generated utilizing an automated platform (Biomek FXP, Beckman Coulter). Both whole-transcriptome amplification and sequencing library preparations were performed in a 96-well format to reduce assay-to-assay variability. Quality control steps were included to determine total RNA quality and quantity, the optimal number of PCR preamplification cycles, and fragment library size [13].

Samples that failed quality controls were eliminated from downstream steps. Libraries that passed strict quality controls were pooled at equimolar concentration, loaded and sequenced on the Illumina Sequencing platform, HiSeq2500 (Illumina). Libraries were sequenced to obtain more than 8 million 50-bp single-end reads (HiSeq Rapid Run Cluster and SBS Kit V2; Illumina) mapping uniquely to mRNA reference, generating a total of ~252 million mapped reads (median of ~8 million filtered mapped reads per sample). Approximately 40% of the total reads were duplicates. Given the inability to separate artifactual read duplicates from true biological duplicates in RNA-sequencing (unlike in DNA sequencing where the initial number of copies is known), we did not filter out duplicate reads during analysis. This approach is consistent with prior studies that show many duplicate reads reflect biological reality and that removal of such duplicates can worsen the power and false discovery rate for differential gene expression [15-16]. The sequences presented in this article have been submitted to Gene Expression Omnibus (http://www.ncbi.nlm.nih.gov/geo/) under accession number GSE128027.

RNA sequencing analysis

RNA-seq data was mapped against the hg38 reference using TopHat [17] (v1.4.1., --librarytype fr-secondstrand -C) and the RefSeq gene annotation downloaded from the UCSC Genome Browser site. The read coverage per gene was computed using HTSeq-count (-m union -s yes -texon -i gene_id,http://www-huber.embl.de/users/anders/HTSeq). To identify genes differentially expressed between GM-CSF, IL-3, and IL-5-stimulated, as well as unstimulated eosinophils, negative binomial tests for pairwise comparisons employing the Bioconductor package DESeq2 (v1.16.1) were performed [18]. Genes were considered differentially expressed between any pairwise comparison when DESeq2 analysis resulted in a Benjamini-Hochberg-adjusted p-value < 0.01 (1% false discovery rate) and $|\text{Log}_2\,(\text{fold change})| \geq 1$. Moreover, any

gene identified as “commonly upregulated” or “commonly downregulated” passed this threshold in all individual pairwise comparisons. Pathway analysis was performed using Ingenuity Pathway Analysis (Qiagen) [19].

Weighted gene co-expression network analysis (WGCNA)

Weighted correlation network analysis using the R package WGCNA (version 1.61) was performed on the transcripts per million data (TPM) matrix [20]. Genes whose expression values were less than 10 TPM in all samples were removed as established in the third phase of the MAQC project (MAQC-III), also called Sequencing Quality Control (SEQC) [21]. A total of 11,889 well-expressed genes were used for generating the co-expression network. A $\beta = 10$ was selected following the scale-free topology criterion [22]. Gene modules were generated using blockwiseModules function (parameters: checkMissingData = TRUE, power = 10, TOMType = "unsigned", minModuleSize = 30, maxBlockSize = 11889, mergeCutHeight = 0.25). A total of 24 different modules were generated, including a ‘grey’ module for non-co-expressed genes which was excluded from further analysis. Since each module by definition is comprised of highly correlated genes, their combined expression may be usefully summarized by eigengene profiles, effectively the first principal component of a given module. A small number of eigengene profiles may therefore summarize the principle patterns within the cellular transcriptome with minimal loss of information. This dimensionality-reduction approach facilitated calculation of a Spearman correlation for modules and each clinical trait (Unstimulated, Stimulated, IL-3, IL-5, GM-CSF) used in the analysis.

To visualize co-expression networks, the function *exportNetworkToCytoscape* at weighted = true, threshold = 0.05 was used. A soft thresholding power was chosen based on the criterion of approximate scale-free topology. Networks were generated in Gephi (version 0.9.2)

using the Fruchterman Reingold layout algorithm followed by Noverlap to eliminate individual node overlap [23]. The size of each gene node was scaled according to the 'average degree' as calculated in Gephi.

Flow cytometry

CD69 and CD131 (CSF2RB) were selected as proteins of interest based on the RNA-sequencing analysis presented in this manuscript and their expression was measured by flow cytometry. Peripheral eosinophils from 6 donors were isolated as described above and stained using specific fluorescently conjugated antibodies: mouse anti-human CD69 coupled to APC-Cy7 (clone FN50, BioLegend) and mouse anti-human CD131 coupled with PE (clone 1C1, BioLegend). Providing 3 biologic replicates, stimulated eosinophils from 3 donors were surface stained with anti-CD69. Similarly, stimulated eosinophils from 3 separate donors were permeabilized using 100% methanol and stained with anti-CD131 (CSF2RB). Flow cytometry data were obtained with a BD Biosciences LSRII, gated to eosinophils using forward and side scatter characteristics in this already highly purified population, and analyzed with FlowJo 10.5.0 Tree Star, Ashland, OR).

Results

β-chain receptor cytokines share common eosinophil activation signals

We first aimed to categorize the transcriptomic profiles distinguishing eosinophils stimulated with β-chain receptor cytokines from those left unstimulated *ex vivo*. Principle component analysis of the 2,000 most variable genes showed clear separation of unstimulated eosinophils from the GM-CSF, IL-3 and IL-5-stimulated groups (Figure 1A). DESeq2 analysis, which assesses for differences in average gene expression across groups, identified differentially expressed genes based on pairwise comparisons among stimulated and unstimulated conditions (Benjamini-Hochberg-adjusted p-value < 0.01). To identify a gene expression profile specific to the stimulated condition ("β-chain receptor cytokine specific genes"), we identified genes for which all pairwise comparisons between the stimulated and unstimulated groups met statistical significance with a Benjamini-Hochberg-adjusted p-value < 0.01 and $|\text{Log}_2(\text{fold change})| \geq 1$. Since DESeq2 does not account for absolute transcript levels and genes exhibiting low expression under stimulated conditions are less likely to have a meaningful biologic effect, we eliminated any gene with less than 10 TPM in a stimulated group. This analysis revealed 252 genes commonly upregulated and 553 genes commonly downregulated by β-chain receptor cytokines (Figure 1B, Supplemental Table I).

Pathway analysis of the commonly upregulated genes revealed multiple pathways utilizing NF-κB signaling, notable for promoting cell survival and proliferation as well as immune mediated inflammation [24]. Of these, the TWEAK (TNFSF12) signaling pathway was most significant (Benjamini-Hochberg-adjusted p-value = 5.49E-07) (Figure 1C). TWEAK is a cytokine belonging to the TNF superfamily and can either be weakly pro-apoptotic by signaling through Death Receptor 3 (DR3/TNFRSF25) or pro-survival and inflammatory by signaling

through Fibroblast Growth Factor-Inducible 14 (Fn14/TNFRSF12A) [25]. We discovered upregulation of *TNFRSF12A* transcripts as well as its downstream signaling mediators (*TRAF3*) and effectors (*NFKB1/NFKB2*) [26]. *BIRC3*, encoding an inhibitor of apoptosis along the TWEAK pathway, was additionally upregulated. Finally, genes commonly upregulated in response to cytokine stimuli were overrepresented in several pathways independent of NF-κB signaling, with the top five pathways including the unfolded protein response (*CD82; CEBPG; INSIG1; NFE2L2; SREBF2*), phagosome maturation (*CTSC; CTSD; CTSL; RAB5A; TUBA1B; TUBA1C; TUBB4B*), tyrosine degradation (*FAH; HPD*), granulocyte adhesion and diapedesis (*CCL1; CCL22; CCL24; CXCL1; ICAM1; IL1A; IL1B*), and 14-3-3 mediated signaling (*ELK1; RRAS; TUBA1B; TUBA1C; TUBB4B; YWHAG*) (Supplemental Table II).

Pathway analysis of the commonly downregulated genes showed an overrepresentation of genes involved in interferon signaling (Figure 1D). We further discovered downregulation of several pro-apoptotic genes including those encoding for the TNF family ligands *TNFSF10* and *FAS*, *CASP3* and the PARP family cleavage products, and the transcription factor *FOXO3* (Supplemental Table II). Collectively, β-chain receptor cytokines stimulate eosinophils to promote a pro-inflammatory and pro-survival phenotype.

IL-3 stimulation yields a unique eosinophil gene expression signature

Similarly focusing on genes that maintained significance in differential expression across all pairwise comparisons, we next aimed to categorize cytokine-specific signals. Supported by IL-3 separation in the principle component analysis (Figure 1A), IL-3 stimulation resulted in the most unique gene expression profile with 158 upregulated genes and 36 downregulated genes relative to all other conditions including unstimulated (Figure 2A, Supplemental Table I). IL-5

analysis revealed one unique downregulated gene (*PMAIP1*) but no upregulated genes. GM-CSF did not produce any unique differentially expressed genes in either direction.

Weighted gene co-expression network analysis (WGCNA), which assigns genes into modules based on similar patterns of change in expression across samples, yielded further support for an IL-3-specific gene expression signal. Of the 24 modules identified by WGCNA, five modules were highly correlated with β-chain receptor cytokine stimulus groups (Figure 2B, $r > 0.5$, $p < 0.01$). The two strongest correlations occurred in relation to IL-3 and are represented by the pink and yellow modules (Figure 2B). These two modules contained 82% of the IL-3 upregulated genes identified by DESeq2 analysis, with most of such genes belonging to the yellow module (Figure 2C). Interestingly, the hub genes of the yellow module were predominantly genes deemed IL-3 specific by DESeq2 analysis (Figure 3, Supplemental Table III, blue nodes/font). Hub genes are the genes that are most tightly co-expressed with other genes within a given module, and therefore, are thought to be key regulators of their corresponding module's biology. The green-yellow and red modules, correlating most strongly with IL-5, and the magenta module, correlating strongly with both GM-CSF and IL-5, also revealed module-specific hub genes but without an overlapping group-specific signal per DESeq2 analysis (Figure 3).

To define the biology of IL-3 stimulation on eosinophils, we focused on the 119 genes that are both differentially upregulated (DESeq2) and highly co-expressed (yellow module) (Figure 2C, Figure 4A). The top hub genes in the yellow module, defined by a module membership $r \geq 0.95$, included 17 genes that were also IL-3 specific by differential expression (Figure 4A, Table I). Included in this cohort were transcripts encoding the common β-chain receptor subunit for GM-CSF, IL-3, and IL-5 (*CSF2RB*), surface activation markers *CD69* and

CD180, two transcriptional regulators extensively linked to the biology of regulatory T cells (*IKZF4, BACH2*), a sulfhydryl oxidase responsible for post-translational disulfide bond formation (*QSOX1*), a regulator of lysosomal dynamics (*TBC1D15*), and a transcription factor required for early eosinophil differentiation (*XBP1*) among other protein coding genes with either known or undefined functions [27-33]. Fluorescence-activating cell sorting (FACS) analysis corroborated our sequencing data at the protein level for two of these genes - *CD69* and *CD131 (CSF2RB)*, and mean fluorescence intensity (MFI) for both markers met statistical significance by one-way ANOVA ($p < 0.05$) (Figure 5). Given that CD69 is a surface marker of leukocyte activation, FACS was performed for surface expression of this protein, while whole cell protein expression was interrogated for CD131 to ensure that any intracellular stores were assayed.

Subsequent pathway analysis of all 119 genes connected to IL-3 by both DESeq2 and WGCNA revealed an overrepresentation of genes involved in JAK/STAT signaling as well as of genes linked to apoptosis mechanisms (Figure 4B, Supplemental Table IV). The later finding contrasts with the collective pro-survival signal we observed in cytokine stimulated eosinophils as a whole. Three non-coding RNAs (*AC090152.1, AC078846.1, LINC01943*) were part of this 119-gene group, and therefore, not recognized by pathway analysis.

Discussion

This study is the first of our knowledge to use two advanced, independent statistical models to analyze whole transcriptome RNA sequencing and categorize the downstream effects of β-chain receptor cytokine signaling. Using an unbiased pathway analysis approach, we discovered an overrepresentation of upregulated pro-survival genes common to all three β-chain receptor cytokines. Genes involved in TWEAK signaling pathway were most enriched. While TWEAK/Fn14 interactions have been connected to several inflammatory diseases including asthma, direct evidence supporting its role in eosinophils is lacking [34-35]. A recent study however linked single nucleotide polymorphisms in *BIRC3*, the inhibitor of apoptosis associated with the TWEAK pathway, with reduced asthma susceptibility and reduced loads of circulating eosinophils [36]. Furthermore, *BIRC3* has been identified as a potential pathogenic gene in childhood asthma based on a molecular interaction network study [37].

Downregulated genes common to all three β-chain receptor cytokines were similarly enriched in several pathways, with the most significant pathway related to interferon signaling. INFα has been demonstrated to inhibit airway eosinophilia and hyperresponsiveness as well as inhibit eosinophil mediator release [38-39]. This finding, together with our observed downregulation of several pro-apoptotic genes, supports a role for inhibition of apoptosis as one method by which β-chain receptor cytokines promote eosinophil's role in asthma pathogenesis.

Most striking in our analysis was the gene expression profile produced by IL-3. Consistent with prior work, we found that IL-3 stimulation most uniquely influences eosinophil gene expression relative to the other β-chain receptor cytokines following prolonged stimulation. Using two independent techniques, we identified a cohort of 119 genes separating IL-3 based both on transcript expression levels and co-expression networks. The top genes in this cohort

included a range of genes with previously described roles in eosinophils, with defined roles in other cell lines but with undescribed function in eosinophils, or with undescribed functions altogether. For instance, XBP1 has been demonstrated as essential for early eosinophil development but less is known about its role in eosinophils that have fully matured in the blood or airway [33]. QSOX1 has gained interest in cancer research as a disulfide bond catalyst with an atypical localization to the Golgi apparatus and extracellular space [30-31]. The importance of such an enzyme in eosinophils may relate to eosinophil disulfide-bond containing secretory proteins (e.g. eosinophil peroxidase and major basic protein) with cytotoxic and immunomodulatory roles in asthma [40-42]. Two transcription factors – IKZF4 and BACH2 – have been connected to regulatory T cell stability, with the later only indirectly linked to eosinophils in the current literature [27-29, 43]. The interaction between CD69 and its ligands (myosin light chains 9 and 12 - the former also a member of our IL-3-defining gene cohort) has been shown to be crucial in allergic airway inflammation and the recruitment of activated T cells to sites of inflammation [44]. Lastly, upregulation of the common β-chain receptor subunit (CSF2RB) may provide a contributing mechanism by which IL-3 uniquely prolongs intracellular signaling in eosinophils [6, 45].

We acknowledge that these 119 genes identified by cytokine stimulation of peripheral blood eosinophils in non-asthmatic subjects may not reflect the true biology of airway eosinophils in asthma patients. In different tissue compartments, eosinophils exist in subsets, each displaying distinct phenotypes and gene expression patterns [46]. While the role of IL-3 stimulation of eosinophils in the airway remains an area of active investigation, there is reason to believe its role is important, particularly in patients who do not respond to anti-IL-5 therapy. Not only does IL-3 increase in the airway of asthmatic subjects following allergen challenge,

eosinophils also display increased levels of surface IL-3 receptor following mepolizumab therapy [5,47]. Esnault et al previously published results of microarray analyses on human BAL and sputum cells following allergen challenge to the lung. Additionally, they assessed for gene downregulation following mepolizumab therapy. Among others, they discovered upregulation in genes that are also members of our IL-3 defining cohort. *CD69, RHOH*, and *ST6GAL1* were upregulated in both BAL and sputum eosinophils subjected to allergen challenge, *IL2RA*, *NDFIP2*, *PIM2*, *SLC2A1*, *SOCS1* and *SVIP* were upregulated in the BAL samples, and *CYTIP*, *IL1RAP*, *MAST4*, *OSBPL3*, *OSM* and *SOCS2* were upregulated in the sputum samples. Of these genes, *CD69*, *NDFIP2* and *SOCS1* were the only to decrease following mepolizumab treatment [48].

We believe the value of our study lies in its genome-wide and unbiased approach. Such methodology allowed us to identify protein-coding genes, some previously associated with asthma, and make novel connections with either IL-3 or the eosinophil cell type. Furthermore, we linked the expression of a few non-coding RNAs to β-chain receptor cytokine stimuli and foresee potential implications as their gene regulatory and epigenetic roles become further defined. These coding and non-coding genes may provide the foundation for future investigation on therapeutic targets in eosinophilic asthma, and with the recognized increase in IL-3-Rα expression in airway eosinophils, may address the current shortcomings of anti-IL-5 therapy. Limitations of our study include the snapshot picture that does not account for the presence of multiple cytokines simultaneously, at varying concentrations over time. Our study of peripheral blood eosinophils from healthy subjects may additionally not account for the effects of the local tissue environment or of the host. Finally, we are limited by the lack of post-transcript analysis,

as prior work has described IL-3 dependent translational modifications that would be missed in the present work [49].

In summary, these results highlight the redundant cytokine signaling mechanisms involved in eosinophil development and function but support a unique role for IL-3. The identification of several genes strongly correlated with IL-3 may provide the foundation for future therapeutic advancements in eosinophilic asthma.

Acknowledgements

We thank the eosinophil donors for their contributions to this project.

References

1. Nurmagambetov, T., R. Kuwahara, and P. Garbe. 2018. The economic burden of asthma in the United States, 2008-2013. *Ann. Am. Thorac. Soc.* 15: 348-356.

2. Bel, E.H., S.E. Wenzel, P.J. Thompson, C.M. Prazma, O.N. Keene, S.W. Yancey, H.G. Ortega, and I.D. Pavord; SIRIUS Investigators. 2014. Oral glucocorticoid-sparing effect of mepolizumab in eosinophilic asthma. *N. Engl. J. Med*. 371: 1189-1197.

3. Ortega, H.G., M.C. Liu, I.D. Pavord, G.G. Brusselle, J.M. FitzGerald, A. Chetta, M. Humbert, L.E. Katz, O.N. Keene, S.W. Yancey, and P. Chanez; MENSA Investigators. 2014. Mepolizumab treatment in patients with severe eosinophilic asthma. *N. Engl. J. Med*. 371: 1198-1207.

4. Flood-Page, P.T., A.N. Menzies-Gow, A.B. Kay, and D.S. Robinson. 2003. Eosinophil's role remains uncertain as anti-interleukin-5 only partially depletes numbers in asthmatic airway. *Am. J. Respir. Crit. Care Med*. 167: 199-204.

5. Kelly, E.A., S. Esnault, L.Y. Liu, M.D. Evans, M.W. Johansson, S. Mathur, D.F. Mosher, L.C. Denlinger, and N.N. Jarjour. 2017. Mepolizumab attenuates airway eosinophil numbers, but not their functional phenotype, in asthma. *Am. J. Respir. Crit. Care Med*. 196: 1385-1395.

6. Esnault, S., and E.A. Kelly. 2016. Essential mechanisms of differential activation of eosinophils by IL-3 compared to GM-CSF and IL-5. *Crit. Rev. Immunol.* 36: 429-444.

7. Asquith, K.L., H.S. Ramshaw, P.M. Hansbro, K.W. Beagley, A.F. Lopez, and P.S. Foster. 2008. The IL-3/IL-5/GM-CSF common receptor plays a pivotal role in the regulation of Th2 immunity and allergic airway inflammation. *J. Immunol.* 180: 1199-1206.

8. Geijsen, N., I.J. Uings, C. Pals, J. Armstrong, M. McKinnon, J.A. Raaijmakers, J.W. Lammers, L. Koenderman, and P.J. Coffer. 2001. Cytokine-specific transcriptional regulation through an IL-5Ralpha interacting protein. *Science*. 293: 1136-1138.

9. Liu, L.Y., J.B. Sedgwick, M.E. Bates, R.F. Vrtis, J.E. Gern, H. Kita, N.N. Jarjour, W.W. Busse, and E.A. Kelly. 2002. Decreased expression of membrane IL-5 receptor alpha on human eosinophils: I. Loss of membrane IL-5 receptor alpha on airway eosinophils and increased soluble IL-5 receptor alpha in the airway after allergen challenge. *J. Immunol.* 169: 6452-6458.

10. Akuthota, P., K. Capron, and P.F. Weller. 2014. Eosinophil purification from peripheral blood. *Methods Mol. Biol.* 1178: 13-20.

11. Seumois, G., P. Vijayanand, C.J. Eisley, N. Omran, L. Kalinke, M. North, A.P. Ganesan, L.J. Simpson, N. Hunkapiller, F. Moltzahn, P.G. Woodruff, J.V. Fahy, D.J. Erle, R. Djukanovic, R. Blelloch, and K.M. Ansel. 2012. An integrated nano-scale approach to profile miRNAs in limited clinical samples. *Am. J. Clin. Exp. Immunol.* 1: 70-89.

12. Seumois, G., L. Chavez, A. Gerasimova, M. Lienhard, N. Omran, L. Kalinke, M. Vedanayagam, A.P. Ganesan, A. Chawla, R. Djukanović, K.M. Ansel, B. Peters, A. Rao, and P. Vijayanand. 2014. Epigenomic analysis of primary human T cells reveals enhancers associated with TH2 memory cell differentiation and asthma susceptibility. *Nat. Immunol.* 15: 777-788.

13. Rosales, S.L., S. Liang, I. Engel, B.J. Schmiedel, M. Kronenberg, P. Vijayanand, and G. Seumois. 2018. A sensitive and integrated approach to profile messenger RNA from samples with low cell numbers. *Methods Mol. Biol.* 1799: 275-301.

14. Picelli, S., O.R. Faridani, A.K. Bjorklund, G. Winberg, S. Sagasser, and R. Sandberg. 2014. Full-length RNA-seq from single cells using Smart-seq2. *Nat. Protoc.* 9: 171-181.

15. Parekh, S., C. Ziegenhain, B. Vieth, W. Enard, and I. Hellmann. 2016. The impact of amplification on differential expression analyses by RNA-seq. *Sci. Rep.* 6: 25533.

16. Fu, Y., P.H. Wu, T. Beane, P.D. Zamore, and Z. Weng. 2018. Elimination of PCR duplicates in RNA-seq and small RNA-seq using unique molecular identifiers. *BMC Genomics.* 19: 531.

17. Trapnell, C., L. Pachter, and S.L. Salzberg. 2009. TopHat: discovering splice junctions with RNA-*Seq*. *Bioinformatics.* 25: 1105-1111.

18. Love, M.I., W. Huber, and S. Anders. 2014. Moderated estimation of fold change and dispersion for RNA-seq data with DESeq2. *Genome Biol.* 15: 550.

19. Krämer, A., J. Green, J. Pollard Jr., and S. Tugendreich. 2014. Causal analysis approaches in Ingenuity Pathway Analysis. *Bioinformatics*. 30: 523-530.

20. Langfelder, P., and S. Horvath. 2008. WGCNA: an R package for weighted correlation network analysis. *BMC Bioinformatics.* 9: 559.

21. Su, Z. ŁP., S. Li, J. Thierry-Mieg, D. Thierry-Mieg, W. Shi, C. Wang, G.P. Schroth, R.A. Setterquist, J.F. Thompson, W.D. Jones, W. Xiao, W. Xu, R.V. Jensen, R. Kelly, J. Xu, A. Conesa, C. Furlanello, H. Gao, H. Hong, N. Jafari, S. Letovsky, Y. Liao, F. Lu, E.J. Oakeley, Z. Peng, C.A. Praul, J. Santoyo-Lopez, A. Scherer, T. Shi, G.K. Smyth, F. Staedtler, P. Sykacek, X.X. Tan, E.A. Thompson, J. Vandesompele, M.D. Wang, J. Wang, R.D. Wolfinger, J. Zavadil, S.S. Auerbach, W. Bao, H. Binder, T. Blomquist, M.H. Brilliant, P.R. Bushel, W. Cai, J.G. Catalano, C.W. Chang, T. Chen, G. Chen, R. Chen, M. Chierici, T.M. Chu, D.A. Clevert, Y. Deng, A. Derti, V. Devanarayan, Z. Dong, J. Dopazo, T. Du, H. Fang, Y. Fang, M. Fasold, A. Fernandez, M. Fischer, P. Furió-Tari, J.C. Fuscoe, F. Caimet, S. Gaj, J. Gandara, H. Gao, W. Ge, Y. Gondo, B. Gong, M. Gong, Z. Gong, B. Green, C. Guo, L. Guo, L.W. Guo, J. Hadfield, J. Hellemans, S. Hochreiter, M. Jia, M. Jian, C.D. Johnson, S. Kay, J. Kleinjans, S. Lababidi, S.

480 Levy, Q.Z. Li, L. Li, L. Li, P. Li, Y. Li, H. Li, J. Li, S. Li, S.M. Lin, F.J. López, X. Lu, H. Luo,
481 X. Ma, J. Meehan, D.B. Megherbi, N. Mei, B. Mu, B. Ning, A. Pandey, J. Pérez-Florido, R.G.
482 Perkins, R. Peters, J.H. Phan, M. Pirooznia, F. Qian, T. Qing, L. Rainbow, P. Rocca-Serra, L.
483 Sambourg, S.A. Sansone, S. Schwartz, R. Shah, J. Shen, T.M. Smith, O. Stegle, N. Stralis-
484 Pavese, E. Stupka, Y. Suzuki, L.T. Szkotnicki, M. Tinning, B. Tu, J. van Delft, A. Vela-Boza, E.
485 Venturini, S.J. Walker, L. Wan, W. Wang, J. Wang, J. Wang, E.D. Wieben, J.C. Willey, P.Y.
486 Wu, J. Xuan, Y. Yang, Z. Ye, Y. Yin, Y. Yu, Y.C. Yuan, J. Zhang, K.K. Zhang, W. Zhang, W.
487 Zhang, Y. Zhang, C. Zhao, Y. Zheng, Y. Zhou, P. Zumbo, W. Tong, D.P. Kreil, C.E. Mason, and
488 L. Shi. 2014. A comprehensive assessment of RNA-seq accuracy, reproducibility and
489 information content by the Sequencing Quality Control Consortium. *Nat. Biotechnol.* 32: 903-
490 914.
491 22. Zhang, B., and S. Horvath. 2005. A general framework for weighted gene co-expression
492 network analysis. *Stat Appl. Genet. Mol. Biol.* 4: Article17.
493 23. Bastian, M., S. Heymann, and M. Jacomy. 2009. Gephi: an open source software for
494 exploring and manipulating networks. International AAAI Conference on Weblogs and Social
495 Media.
496 24. Gupta, S.C., C. Sundaram, S. Reuter, and B.B. Aggarwal. 2010. Inhibiting NF-KB activation
497 by small molecules as a therapeutic strategy. *Biochim. Biophys. Acta.* 1799: 775-787.
498 25. Burkly, L.C., J.S. Michaelson, K. Hahm, A. Jakubowski, and T.S. Zheng. 2007. TWEAKing
499 tissue remodeling by a multifunctional cytokine: role of TWEAK/Fn14 pathway in health and
500 disease. *Cytokine.* 40: 1-16.
501 26. Bhattacharjee, M., R. Raju, A. Radhakrishnan, V. Nanjappa, B. Muthusamy, K. Singh, D.
502 Kuppusamy, B.T. Lingala, A. Pan, P.P. Mathur, H.C. Harsha, T.S. Prasad, G.J. Atkins, A.

503 Pandey, and A. Chatterjee. 2012. A bioinformatics resource for TWEAK-Fn14 signaling
504 pathway. *J. Signal Transduct*. 2012: 376470.
505 27. Pan, F., H. Yu, E.V. Dang, J. Barbi, X. Pan, J.F. Grosso, D. Jinasena, S.M. Sharma, E.M.
506 McCadden, D. Getnet, C.G. Drake, J.O. Liu, M.C. Ostrowski, and D.M. Pardoll. 2009. Eos
507 mediates Foxp3-dependent gene silencing in CD4+ regulatory T cells. *Science.* 325: 1142-1146.
508 28. Roychoudhuri, R., K. Hirahara, K. Mousavi, D. Clever, C.A. Klebanoff, M. Bonelli, G.
509 Sciumè, H. Zare, G. Vahedi, B. Dema, Z. Yu, H. Liu, H. Takahashi, M. Rao, P. Muranski, J.G.
510 Crompton, G. Punkosdy, D. Bedognetti, E. Wang, V. Hoffmann, J. Rivera, F.M. Marincola, A.
511 Nakamura, V. Sartorelli, Y. Kanno, L. Gattinoni, A. Muto, K. Igarashi, J.J. O'Shea, and N.P.
512 Restifo. 2013. BACH2 represses effector programs to stabilize T(reg)-mediated immune
513 homeostasis. *Nature.* 498: 506-510.
514 29. Yu, X., Y. Lao, X.L. Teng, S. Li, Y. Zhou, F. Wang, X. Guo, S. Deng, Y. Chang, X. Wu, Z.
515 Liu, L. Chen, L.M. Lu, J. Cheng, B. Li, B. Su, J. Jiang, H.B. Li, C. Huang, J. Yi, and Q. Zou.
516 2018. SENP3 maintains the stability and function of regulatory T cells via BACH2
517 deSUMOylation. *Nat. Commun.* 9: 3157.
518 30. Alon, A., I. Grossman, Y. Gat, V.K. Kodali, F. DiMaio, T. Mehlman, G. Haran, D. Baker, C.
519 Thorpe, and D. Fass. 2012. The dynamic disulfide relay of quiescin sulphydryl oxidase. *Nature.*
520 488: 414-418.
521 31. Ilani, T., A. Alon, I. Grossman, B. Horowitz, E. Kartvelishvily, S.R. Cohen, and D. Fass.
522 2013. A secreted disulfide catalyst controls extracellular matrix composition and function.
523 *Science.* 341: 74-76.
524 32. Wong, Y.C., D. Ysselstein, and D. Krainc. 2018. Mitochondria-lysosome contacts regulate
525 mitochondrial fission via RAB7 GTP hydrolysis. *Nature.* 554: 382-386.

526 33. Bettigole, S.E., R. Lis, S. Adoro, A.H. Lee, L.A. Spencer, P.F. Weller, and L.H. Glimcher.
527 2015. The transcription factor XBP1 is selectively required for eosinophil differentiation. *Nat.*
528 *Immunol.* 16: 829-837.
529 34. Sidler, D., P. Wu, R. Herro, M. Claus, D. Wolf, Y. Kawakami, T. Kawakami, L. Burkly, and
530 M. Croft. 2017. TWEAK mediates inflammation in experimental atopic dermatitis and psoriasis.
531 *Nat. Commun.* 8: 15395.
532 35. Zhu, C., L. Zhang, Z. Liu, C. Li, and Y. Bai. 2018. TWEAK/Fn14 interaction induces
533 proliferation and migration in human airway smooth muscle cells via activating the NF-KB
534 pathway. *J. Cell Biochem.* 119: 3528-3536.
535 36. Roscioli, E., R. Hamon, R.E. Ruffin, J. Grant, S. Hodge, P. Zalewski, and S. Lester. 2017.
536 BIRC3 single nucleotide polymorphism associate with asthma susceptibility and the abundance
537 of eosinophils and neutrophils. *J. Asthma.* 54: 116-124.
538 37. Gao, X.M. 2016. A network approach predicts NFKBIA and BIRC3 as pathogenic genes in
539 childhood asthma. *Genet. Mol. Res.* 15.
540 38. Kikkawa, Y., K. Sugiyama, K. Obara, H. Hirata, Y. Fukushima, M. Toda, and T. Fukuda.
541 2012. Interferon-alpha inhibits airway eosinophilia and hyperresponsiveness in an animal asthma
542 model. *Asia Pac. Allergy.* 2: 256-263.
543 39. Aldebert, D., B. Lamkhioued, C. Desaint, A.S. Gounni, M. Goldman, A. Capron, L. Prin, and
544 M. Capron. 1996. Eosinophils express a functional receptor for interferon alpha: inhibitory role
545 of interferon alpha on the release of mediators. *Blood*. 87: 2354-2360.
546 40. Wagner, L.A., L.E. Ohnuki, K. Parsawar, G.J. Gleich, and C.C. Nelson. 2007. Human
547 eosinophil major basic protein 2: location of disulfide bonds and free sulfhydryl groups. *Protein*
548 *J.* 26: 13-18.

549 41. Thomsen, A.R., L. Sottrup-Jensen, G.J. Gleich, and C. Oxvig. 2000. The status of half-
550 cystine residues and locations on N-glycosylated asparagine residues in human eosinophil
551 peroxidase. *Arch. Biochem. Biophys.* 379: 147-152.
552 42. McBrien, C.N., and A. Menzies-Gow. 2017. The biology of eosinophils and their role in
553 asthma. *Front. Med.* 4: 93.
554 43. Sato, Y., H. Kato, R. Ebina-Shibuya, A. Itoh-Nakadai, R. Okuyama, and K. Igarashi. 2017.
555 Bach2 controls homeostasis of eosinophils by restricting the type-2 helper function of T cells.
556 *Tohoku J. Exp. Med.* 241: 175-182.
557 44. Hayashizaki, K., M.Y. Kimura, K. Tokoyoda, H. Hosokawa, K. Shinoda, K. Hirahara, T.
558 Ichikawa, A. Onodera, A. Hanazawa, C. Iwamura, J. Kakuta, K. Muramoto, S. Motohashi, D.J.
559 Tumes, T. Iinuma, H. Yamamoto, Y. Ikehara, Y. Okamoto, and T. Nakayama. 2016. Myosin
560 light chains 9 and 12 are functional ligands for CD69 that regulate airway inflammation. *Sci.*
561 *Immunol.* 1 :1-10.
562 45. Esnault, S., A.S. Hebert, N.N. Jarjour, J.J. Coon, and D.F. Mosher. 2018. Proteomic and
563 phospho-proteomic changes induced by prolonged activation of human eosinophils with IL-3. J.
564 *Proteome Res.* 17: 2102-2111.
565 46. Mesnil, C., S. Raulier, G. Paulissen, X. Xiao, M.A. Birrell, D. Pirottin, T. Janss, P. Starkl, E.
566 Ramery, M. Henket, F.N. Schleich, M. Radermecker, K. Thielemans, L. Gillet, M. Thiry, M.G.
567 Belvisi, R. Louis, C. Desmet, T. Marichal, and F. Bureau. 2016. Lung-resident eosinophils
568 represent a distinct regulatory eosinophil subset. *J. Clin. Invest.* 126: 3279-3295.
569 47. Johansson, M.W., E.A. Kelly, W.W. Busse, N.N. Jarjour, and D.F. Mosher. 2008. Up-
570 regulation and activation of eosinophil integrins in blood and airway after segmental lung
571 antigen challenge. *J. Immunol.* 180: 7622-7635.

48. Esnault, S., E.A. Kelly, E.A. Schwantes, L.Y. Liu, L.P. DeLain, J.A. Hauer, Y.A. Bochkov, L.C. Denlinger, J.S. Malter, S.K. Mathur, and N.N. Jarjour. 2013. Identification of genes expressed by human airway eosinophils after an in vivo allergen challenge. *PLoS One.* 8: e67560.

49. Esnault, S., E.A. Kelly, M.W. Johansson, L.Y. Liu, S-H. Han, M. Akhtar, N Sandbo, D.F. Mosher, L.C. Denlinger, S.K. Mathur, J.S. Malter, and N.N. Jarjour. 2014. Semaphorin 7A is expressed on airway eosinophils and upregulated by IL-5 family cytokines. *Clin. Immunol.* 150: 90–100.

Footnotes

Grant Support: This work was supported by National Institutes of Health Grants NIH K08HL116429 (P.A.) and NIH S10OD016262 (G.S.).

Abbreviations: TPM: transcripts per million, WGCNA: weighted gene co-expression network analysis

Correspondence Address: 9500 Gilman Dr., MC 7381, La Jolla, CA 92037

Conflict of Interest: The authors whose names are listed certify that they have no financial or non-financial interests in the subject matter or materials discussed in this manuscript.

Figure Legends

Figure 1. β-chain receptor cytokines share common activation signals on eosinophils.

A. tSNE plot of the top 2000 differentially expressed genes (5 principle components; 9 perplexity) **B.** Heatmap depicting the 252 commonly upregulated and 553 commonly downregulated genes in response to β-chain receptor cytokine stimulation. **C,D**. Top 10 pathways represented by the commonly upregulated and downregulated genes. The number of genes identified by differential expression analysis in relation to the total number of genes known for any given pathway are represented by percentages.

Figure 2. IL-3 stimulation yields a unique eosinophil gene expression signature.

A. Heatmap depicting the 158 upregulated and 36 downregulated genes in response to IL-3 stimulation. **B.** Select WGCNA modules reaching significance ($p < 0.01$). Numerical cells indicate the Spearman correlation coefficient of the stimulus group to the module. **C.** Genes similarly identified by DESeq2 and WGCNA analysis.

Figure 3. Hub genes of the yellow WGCNA module include a large number of differentially expressed IL-3 specific genes

Gene connectivity plots of the five significant WGCNA modules along with the mean gene expression for the most representative ("hub") gene of each module. Top 10% of genes from each module are shown. Large nodes indicate "hub genes" of increased connectivity. Blue nodes represent genes that were group-specific based on DESeq2 analysis. For example, in the yellow module nodes that are depicted in blue rather than yellow represent IL-3 specific genes based on DESeq2 analysis. In this particular module, there were a large number of IL-3 specific differentially expressed genes amongst the WGCNA hub genes. Error bars indicate standard error of the mean.

Figure 4. IL-3 stimulation yields 119 differentially expressed and highly co-expressed genes

A. Genes both differentially upregulated (DESeq2 analysis) and highly co-expressed (yellow module) following IL-3 stimulation (n=119). **B.** Pathway enrichment analysis of these 119 genes.

Figure 5. Protein levels of CD69 and CD131 in human eosinophils

Fluorescence-activated cell sorting (FACS) of surface CD69 and total cell CD131 (CSF2RB) with mean fluorescence intensity (MFI) for each cytokine-stimulated condition. Both met statistical significance by one-way ANOVA ($p < 0.05$). Corresponding sequencing data for each gene is included in transcripts per million (TPM).

File type: Figure
Label: 1
File name: figure_1.tif

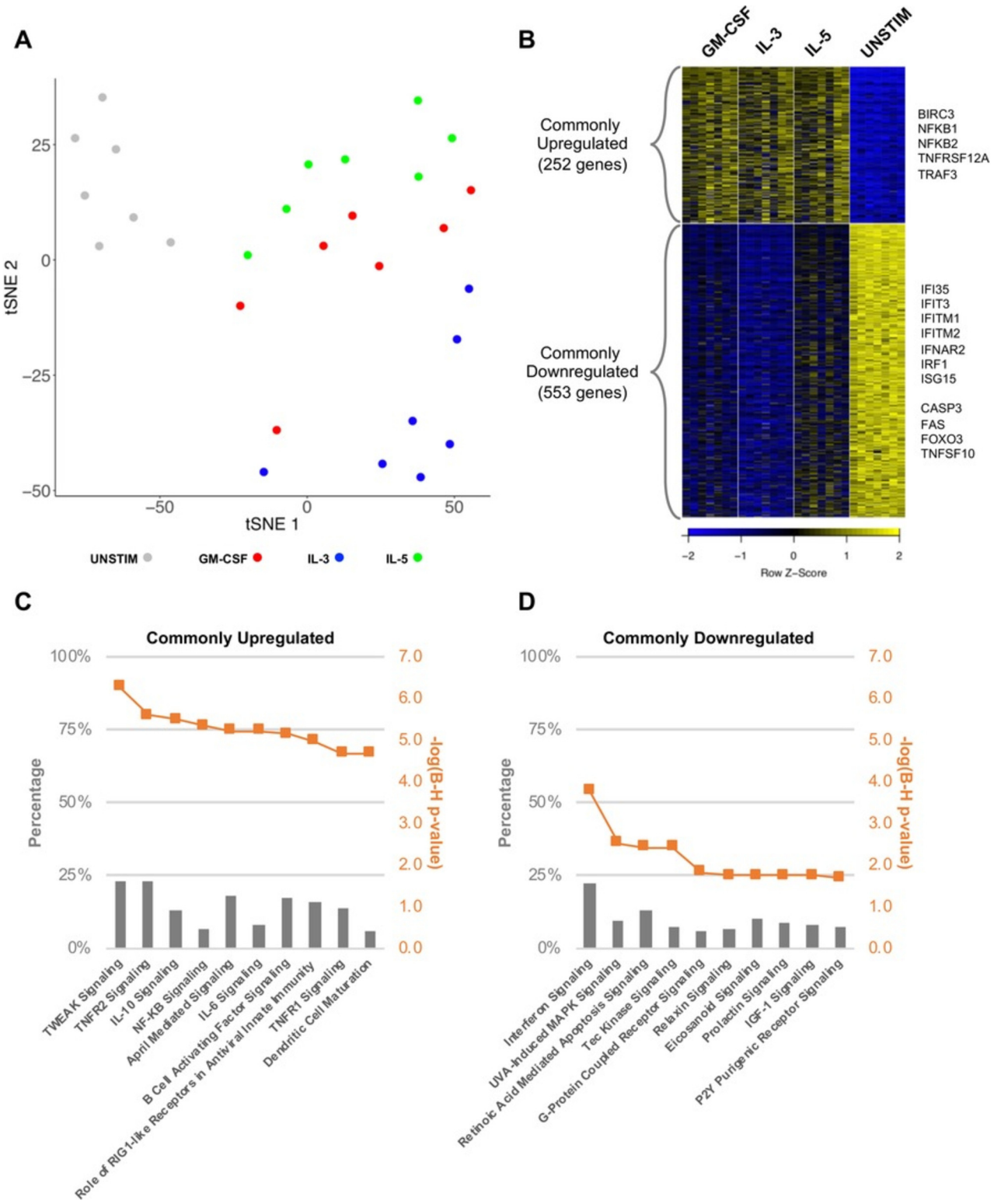
A
tSNE 2
tSNE 1
UNSTIM
GM-CSF
IL-3
IL-5
B
GM-CSF
IL-3
IL-5
UNSTIM
Commonly Upregulated (252 genes)
Commonly Downregulated (553 genes)
BIRC3
NFKB1
NFKB2
TNFRSF12A
TRAF3
IFI35
IFIT3
IFITM1
IFITM2
IFNAR2
IRF1
ISG15
CASP3
FAS
FOXO3
TNFSF10
Row Z-Score
C
Commonly Upregulated
Percentage
-log(B-H p-value)
TWEAK Signaling
TNFR2 Signaling
IL-10 Signaling
NF-KB Signaling
April Mediated Signaling
IL-6 Signaling
B Cell Activating Factor Signaling
Role of RIG1-like Receptors in Antiviral Innate Immunity
TNFR1 Signaling
Dendritic Cell Maturation
D
Commonly Downregulated
Percentage
-log(B-H p-value)
Interferon Signaling
UVA-Induced MAPK Signaling
Retinoic Acid Mediated Apoptosis Signaling
Tec Kinase Signaling
G-Protein Coupled Receptor Signaling
Relaxin Signaling
Eicosanoid Signaling
Prolactin Signaling
IGF-1 Signaling
P2Y Purigenic Receptor Signaling

File type: Figure
Label: 2
File name: figure_2.tif

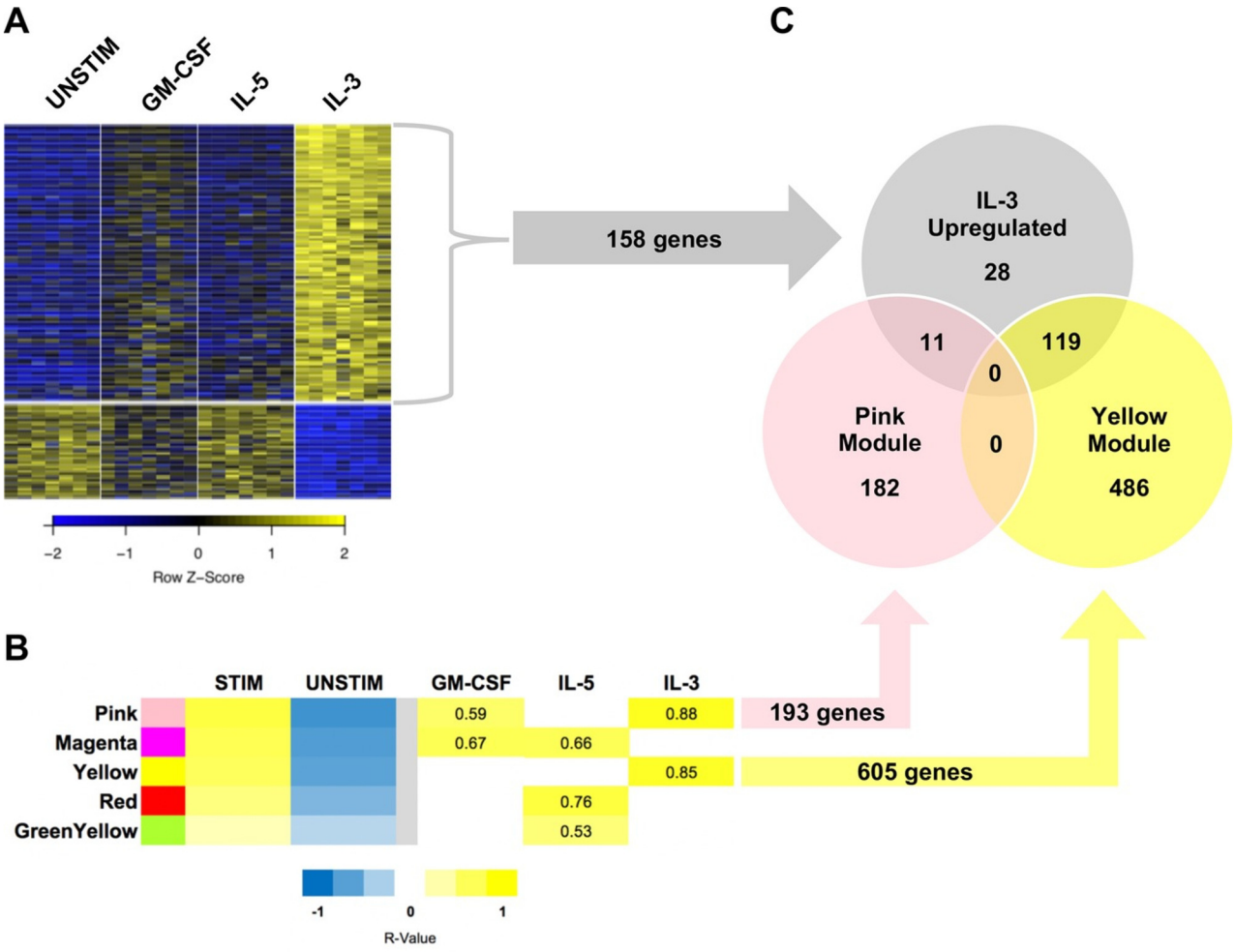
A
UNSTIM
GM-CSF
IL-5
IL-3
−2
−1
0
1
2
Row Z−Score
158 genes
C
IL-3
Upregulated
28
11
119
0
Pink
Module
182
0
Yellow
Module
486
B
STIM
UNSTIM
GM-CSF
IL-5
IL-3
Pink
Magenta
Yellow
Red
GreenYellow
0.59
0.88
0.67
0.66
0.85
0.76
0.53
193 genes
605 genes
-1
0
1
R-Value

File type: Figure
Label: 3
File name: figure_3.tif

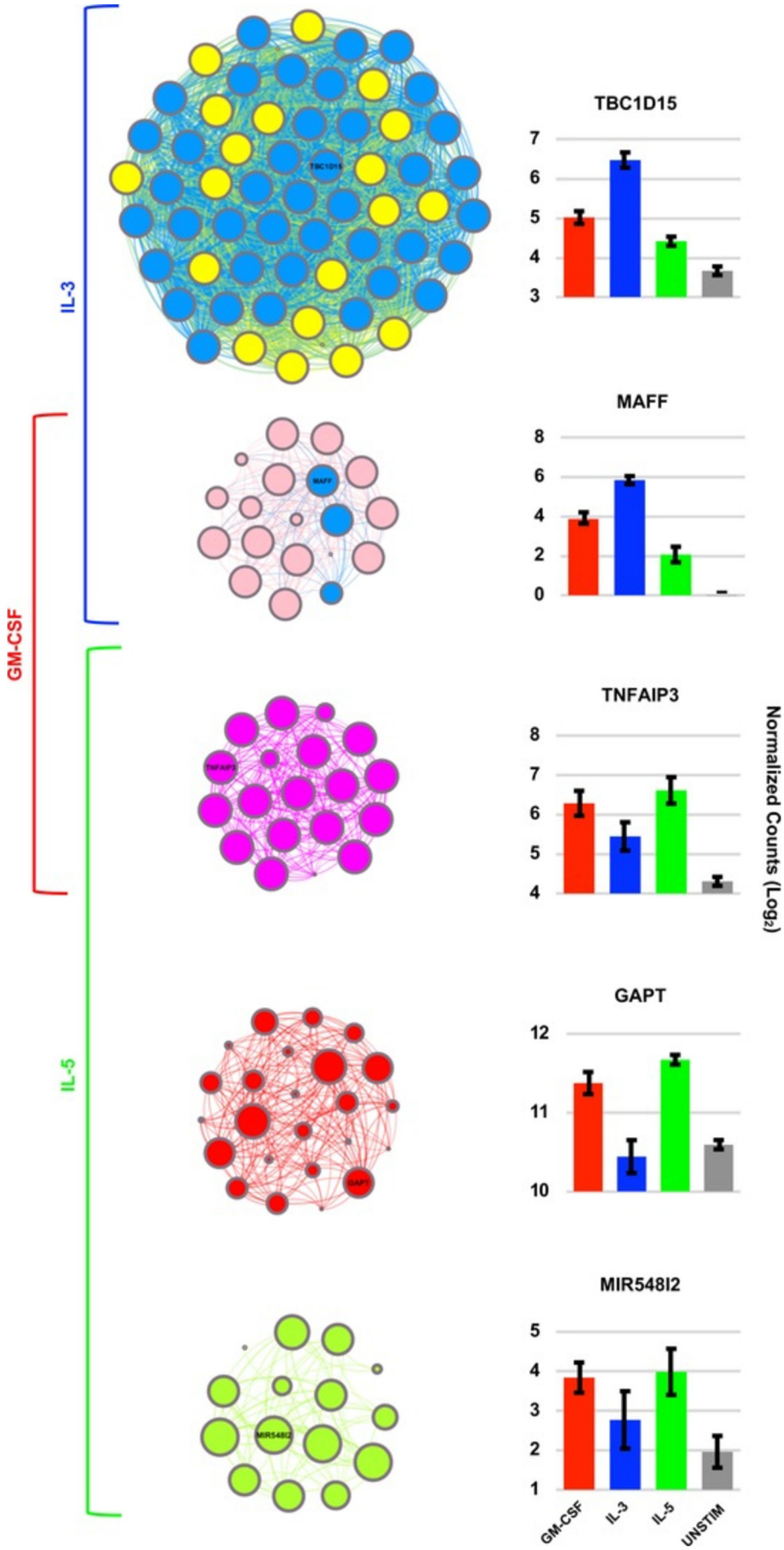
IL-3
GM-CSF
IL-5
TBC1D15
MAFF
TNFAIP3
GAPT
MIR548I2
Normalized Counts (Log2)
GM-CSF
IL-3
IL-5
UNSTIM

File type: Figure
Label: 4
File name: figure_4.tif

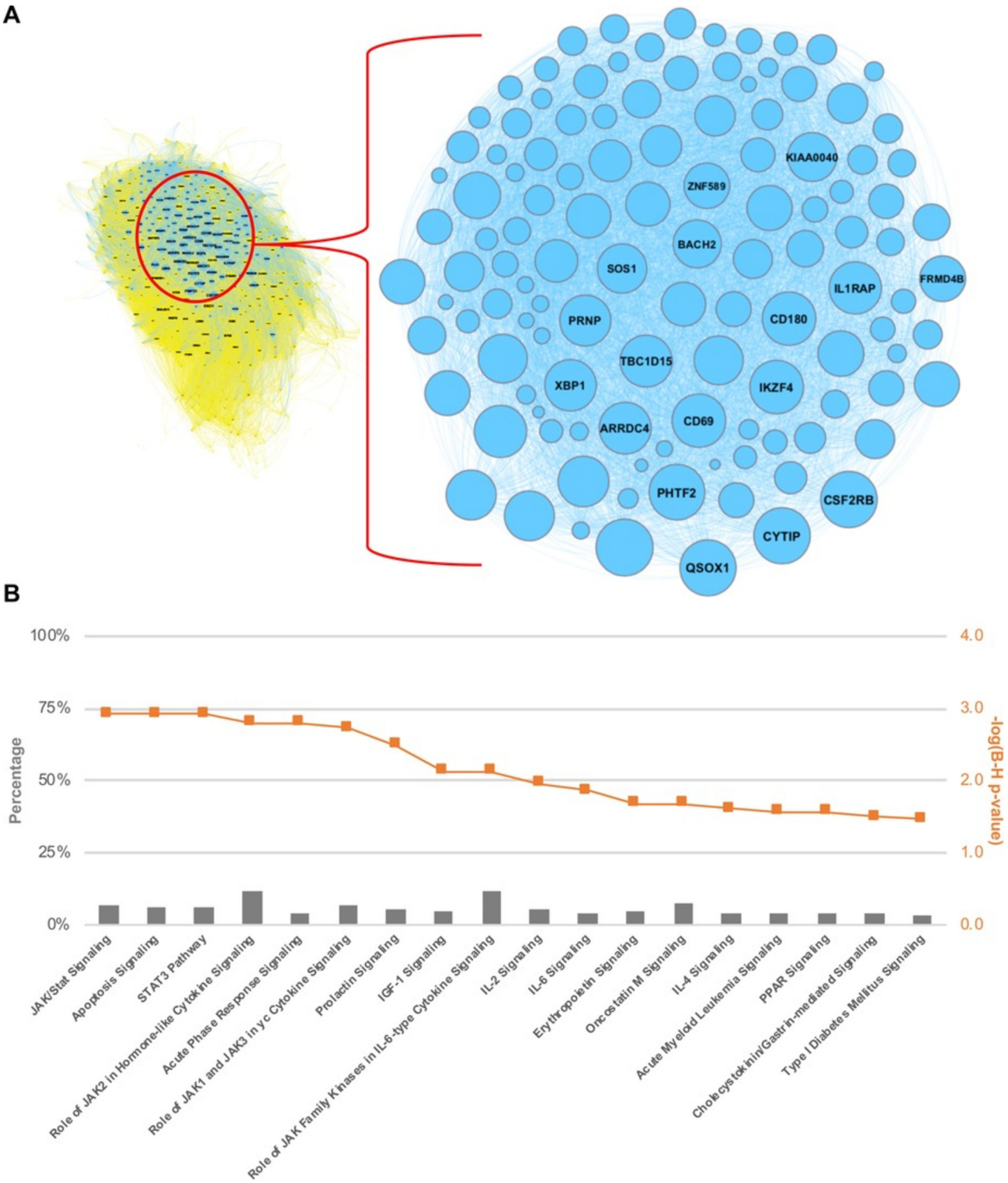
A
KIAA0040
ZNF589
BACH2
SOS1
IL1RAP
FRMD4B
PRNP
CD180
TBC1D15
XBP1
IKZF4
ARRDC4
CD69
PHTF2
CSF2RB
CYTIP
QSOX1
B
100%
75%
50%
25%
0%
Percentage
4.0
3.0
2.0
1.0
0.0
-log(B-H p-value)
JAK/Stat Signaling
Apoptosis Signaling
STAT3 Pathway
Role of JAK2 in Hormone-like Cytokine Signaling
Acute Phase Response Signaling
Role of JAK1 and JAK3 in γc Cytokine Signaling
Prolactin Signaling
IGF-1 Signaling
Role of JAK Family Kinases in IL-6-type Cytokine Signaling
IL-2 Signaling
IL-6 Signaling
Erythropoietin Signaling
Oncostatin M Signaling
IL-4 Signaling
Acute Myeloid Leukemia Signaling
PPAR Signaling
Cholecystokinin/Gastrin-mediated Signaling
Type I Diabetes Mellitus Signaling

File type: Figure
Label: 5
File name: figure_5.tif

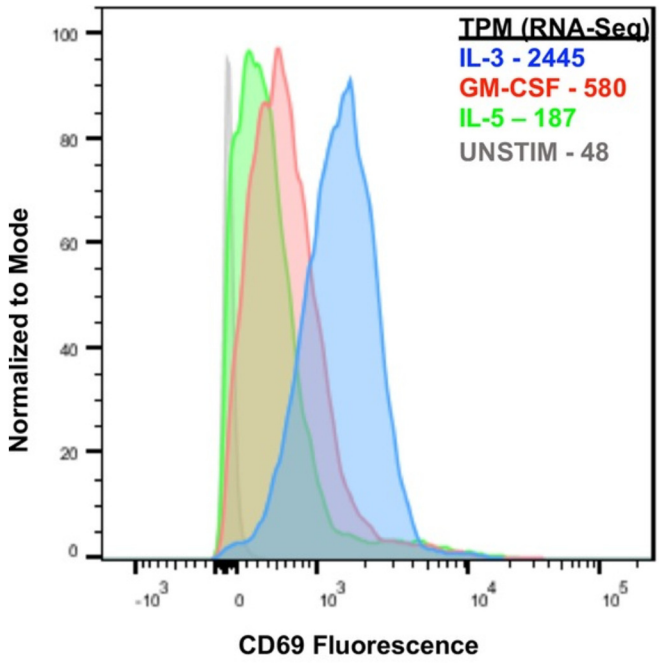
TPM (RNA-Seq)
IL-3 - 2445
GM-CSF - 580
IL-5 – 187
UNSTIM - 48
Normalized to Mode
CD69 Fluorescence

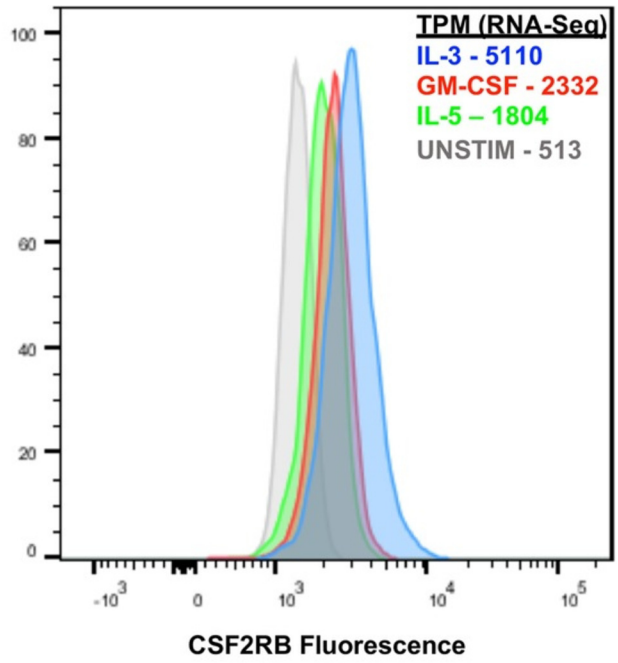
TPM (RNA-Seq)
IL-3 - 5110
GM-CSF - 2332
IL-5 – 1804
UNSTIM - 513
CSF2RB Fluorescence

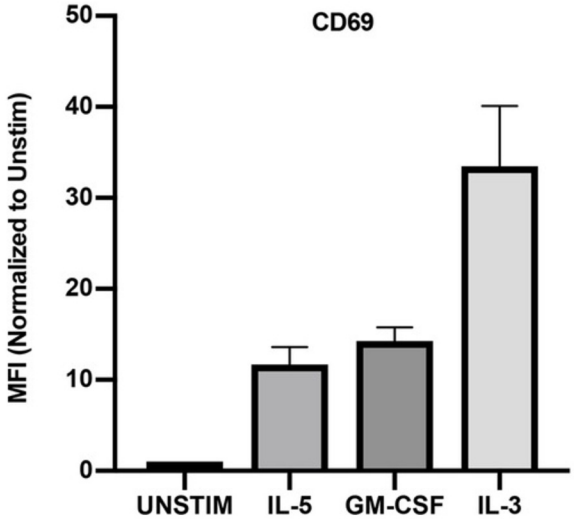
CD69
MFI (Normalized to Unstim)
UNSTIM
IL-5
GM-CSF
IL-3

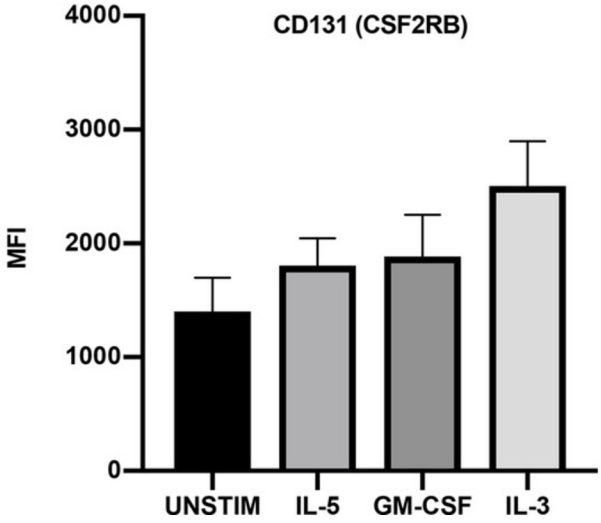
CD131 (CSF2RB)
MFI
UNSTIM
IL-5
GM-CSF
IL-3

File type: Table
Label: 1
File name: table_1.doc

Gene Symbol	Gene Significance (IL-3)		Module Membership		Normalized Mean Counts			
	GS (r)	P-Value	MM (r)	P-Value	GM-CSF	IL-3	IL-5	UNSTIM
TBC1D15	0.82	1.06E-07	0.98	5.06E-19	33	93	22	13
CD180	0.81	1.65E-07	0.97	4.33E-18	48	287	6	2
CD69	0.82	8.02E-08	0.97	5.24E-18	580	2445	187	48
IL1RAP	0.77	1.75E-06	0.97	1.23E-17	54	169	35	26
IKZF4	0.85	1.30E-08	0.97	8.24E-17	17	69	7	1
QSOX1	0.90	9.91E-11	0.96	2.89E-16	55	137	42	14
ARRDC4	0.82	1.09E-07	0.96	3.87E-16	144	546	51	55
PHTF2	0.91	3.48E-11	0.96	6.65E-16	70	159	56	17
SOS1	0.84	2.10E-08	0.96	8.23E-16	30	89	25	10
KIAA0040	0.79	7.47E-07	0.95	3.74E-15	34	120	23	12
BACH2	0.79	6.24E-07	0.95	3.79E-15	2	14	2	1
FRMD4B	0.73	9.13E-06	0.95	8.55E-15	15	69	11	3
CSF2RB	0.86	5.37E-09	0.95	1.90E-14	2332	5110	1804	513
PRNP	0.86	6.73E-09	0.95	2.19E-14	135	598	104	38
XBP1	0.86	3.20E-09	0.95	2.90E-14	241	572	151	96
ZNF589	0.79	5.07E-07	0.95	3.52E-14	9	33	6	6
CYTIP	0.87	1.25E-09	0.95	3.64E-14	756	1554	567	248

Table I. IL-3 specific hub genes

Top hub genes of the yellow module as defined by a correlation coefficient ≥ 0.95. All 17 genes were also IL-3 specific based on DESeq2 analysis.